

Millimeter-Wave-Band Amplifier and Mixer MMIC's Using a Broad-Band 45° Power Divider/Combiner

Hitoshi Hayashi, *Member, IEEE*, Hiroshi Okazaki, *Associate Member, IEEE*, Atsushi Kanda, *Member, IEEE*, Tetsuo Hirota, *Member, IEEE*, and Masahiro Muraguchi, *Member, IEEE*

Abstract— This paper demonstrates millimeter-wave-band amplifier and mixer monolithic microwave integrated circuits (MMIC's) using a broad-band 45° power divider/combiner. At first, we propose a broad-band 45° power divider/combiner, which combines a Wilkinson divider/combiner, 45° delay line, and 90° short stub. A coupling loss of 4.0 ± 0.2 dB and a return loss and an isolation of more than 19 dB with 45 ± 1 ° phase difference was obtained from 17 to 22 GHz for the fabricated K-band MMIC 45° power divider/combiner. Next, a parallel amplifier using the broad-band 45° power divider/combiner, which can be used in a power-combining circuit configuration requiring no isolator, is shown. Comparing the transmitter intermodulation generated in the parallel amplifier using the broad-band 45° power divider/combiner and that generated in the one using the conventional type, the broad-band suppression effect was confirmed. Finally, an application of the broad-band 45° power divider/combiner to a single-sideband (SSB) subharmonically pumped (SHP) mixer requiring no IF switch is shown. In an RF frequency range from 22.89 to 26.39 GHz, the fabricated K-band MMIC mixer achieved (for up-conversion) the good results of more than -13 -dB conversion gain and more than 24-dB image-rejection ratio. These contribute significantly to the miniaturization of millimeter-wave communication equipment.

Index Terms— Millimeter-wave amplifiers, millimeter-wave circuits, millimeter-wave mixers, millimeter-wave technology, MMIC's, power amplifiers.

I. INTRODUCTION

MILLIMETER-WAVE communication systems have been attracting attention because they are able to offer wide bandwidth for achieving the high bit rates and large capacity needed in the multimedia age [1]. In these systems, it is necessary for the equipment to be compact, lightweight, and low-cost. In order to satisfy these requirements, the application of monolithic microwave integrated circuit (MMIC) technology to millimeter-wave circuits is highly desirable. Furthermore, in order to promote the miniaturization of the circuit, a circuit configuration requiring no isolator, filter, or switch, which together take up a large area, should be adopted.

We have previously proposed an amplifier configuration which reduces the transmitter intermodulation without in-

serting an isolator between the RF circuit and the antenna [2]–[4]. This configuration uses a combination of parallel amplifiers—one using a 90° divider/combiner and one using a 45° divider/combiner. We then fabricated a K-band experimental unit amplifier, a parallel amplifier using 90° hybrids, and one using a 45° divider/combiner fabricated with simple 45° delay line. From the comparison of spectra of these amplifiers, the feasibility of constructing a parallel amplifier capable of entirely cancelling all of the generated intermodulation was confirmed. However, since the simple 45° delay line was used for the fabricated experimental parallel amplifier in order to make the 45° phase difference, the frequency range where about 45° phase difference can be achieved was narrow. In order to attain maximum performance from the proposed circuit configuration, a parallel amplifier using a broad-band 45° divider/combiner must be adopted.

Furthermore, we have previously proposed a single-sideband (SSB) subharmonically pumped (SHP) mixer requiring no IF switch [5]. The phase imbalance of LO power has a significant influence on the image-rejection ratio of the SSB mixer, while the amplitude imbalance of LO power has little effect on it, considering the LO power dependence of the SHP mixer. Thus, the broad-band 45° divider is needed for the LO 45° divider in order to obtain the good image-rejection ratio.

This paper reports on the broad-band 45° power divider/combiner and its application to millimeter-wave amplifier and mixer MMIC's. To the best of the authors' knowledge, there have been few reports about the broad-band 45° power divider/combiner applied to millimeter-wave-band circuits, while there have been many reports about the millimeter-wave broad-band 90° power divider/combiner [6]–[9].

II. BROAD-BAND 45° POWER DIVIDER/COMBINER

The circuit configuration of the conventional 45° power divider/combiner is shown in Fig. 1(a). A 45° phase difference is made by combining a Wilkinson divider/combiner and a delay line with an electrical length of 45° at the frequency f_0 . This configuration is attractive because of its simplicity and easy fabrication. However, since the electrical length of the delay line is in proportion to operating frequency, it cannot maintain the phase difference of about 45° with a broad-band frequency range.

In order to realize a broad-band 45° power divider/combiner, we have inserted a short stub with an electrical length of 90° at the frequency f_0 to the side opposite the 45°

Manuscript received October 15, 1997; revised March 4, 1998.

H. Hayashi, H. Okazaki, A. Kanda, and M. Muraguchi are with NTT Wireless Systems Laboratories, Yokosuka-shi, Kanagawa 239, Japan.

T. Hirota was with NTT Wireless Systems Laboratories, Yokosuka-shi, Kanagawa 239, Japan. He is now with NTT Mobile Communications Network Inc., Minato-ku, Tokyo 105, Japan.

Publisher Item Identifier S 0018-9480(98)04045-9.

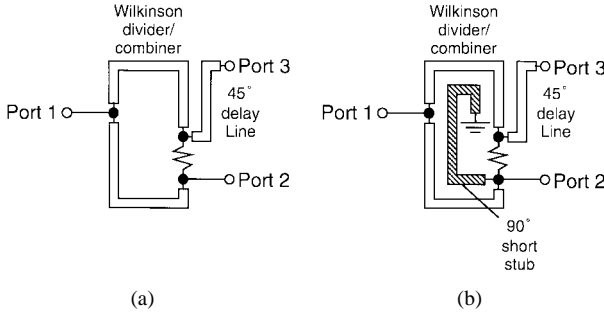


Fig. 1. 45° power divider/combiner. (a) Conventional type. (b) Proposed type.

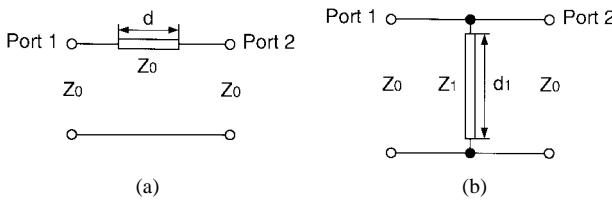


Fig. 2. Calculation of the scattering matrix. (a) Delay line. (b) Short stub.

delay line, as shown in Fig. 1(b). Note that this stub can be fabricated within the area of the Wilkinson divider/combiner, and the combined area is as small as the conventional type. This stub acts as a phase deviation compensation circuit. In this case, the input impedance of the short stub is infinite at the frequency f_0 . Then, by determining the parameters of the short stub so that the transmission-phase variations of the delay line and the short stub near frequency f_0 are almost the same, it is possible to compensate the phase deviation between $\text{phase}(S_{21})$ and $\text{phase}(S_{31})$. The parameters are determined as follows.

Assuming that the characteristic impedances of input and output ports are Z_0 , the scattering matrix of the transmission line with characteristic impedance Z_0 and length d , shown in Fig. 2(a), is expressed by

$$\begin{bmatrix} 0 & \frac{1}{\cos \beta(\omega)d + j \sin \beta(\omega)d} \\ \frac{1}{\cos \beta(\omega)d + j \sin \beta(\omega)d} & 0 \end{bmatrix} \quad (1)$$

in which the angular frequency and the phase constant are expressed as ω and $\beta(\omega)$, respectively. From (1), $\text{phase}(S_{21})$ is expressed as follows:

$$\text{phase}(S_{21}) = -\beta(\omega)d. \quad (2)$$

Then, the differential coefficient of $\text{phase}(S_{21})$ at an angular frequency of ω_0 is expressed as follows:

$$\frac{\partial \text{phase}(S_{21})}{\partial \omega} \Big|_{\omega_0} = -d \frac{\partial \beta(\omega)}{\partial \omega} \Big|_{\omega_0}. \quad (3)$$

Assuming that $\beta(\omega)$ is in proportion to ω , the following equation holds well:

$$\frac{\partial \beta(\omega)}{\partial \omega} \Big|_{\omega_0} = \frac{\beta(\omega_0)}{\omega_0}. \quad (4)$$

Then, (3) is expressed as follows:

$$\frac{\partial \text{phase}(S_{21})}{\partial \omega} \Big|_{\omega_0} = -\frac{\beta(\omega_0)d}{\omega_0}. \quad (5)$$

Next, assuming that the characteristic impedances of input and output ports are Z_0 , the scattering matrix of the short stub with characteristic impedance Z_1 and length d_1 , shown in Fig. 2(b), is expressed by

$$\begin{bmatrix} -1 & \frac{1}{1 - j \left\{ \frac{Z_0}{2Z_1} \tan \beta(\omega)d_1 \right\}} \\ \frac{1}{1 - j \left\{ \frac{Z_0}{2Z_1} \tan \beta(\omega)d_1 \right\}} & \frac{1}{1 + j \left\{ \frac{2Z_1}{Z_0} \tan \beta(\omega)d_1 \right\}} \end{bmatrix}. \quad (6)$$

From (6), $\text{phase}(S_{21})$ is expressed as follows:

$$\text{phase}(S_{21}) = \text{arc tan} \left\{ \frac{Z_0}{2Z_1} \frac{1}{\tan \beta(\omega)d_1} \right\}. \quad (7)$$

Its value is zero at an angular frequency of ω_0 , at which the following equation holds well:

$$\beta(\omega_0)d_1 = \pi/2. \quad (8)$$

Then, the following equation holds well at angular frequency ω near ω_0 :

$$\text{phase}(S_{21}) \cong \frac{Z_0}{2Z_1} \frac{1}{\tan \beta(\omega)d_1}. \quad (9)$$

The differential coefficient of $\text{phase}(S_{21})$ at angular frequency ω_0 is expressed as follows:

$$\frac{\partial \text{phase}(S_{21})}{\partial \omega} \Big|_{\omega_0} = -\frac{Z_0}{2Z_1} d_1 \frac{\partial \beta(\omega)}{\partial \omega} \Big|_{\omega_0}. \quad (10)$$

Thus, the condition of minimal variation of phase deviation at frequency f_0 is that (3) and (10) become equal, i.e., that the following equation holds well:

$$\frac{d}{d_1} = \frac{Z_0}{2Z_1}. \quad (11)$$

Assuming that

$$d = \frac{d_1}{2} \quad (12)$$

(11) is rewritten as follows:

$$Z_1 = Z_0. \quad (13)$$

Next, a broad-band 45° power divider/combiner using a short stub was fabricated on a GaAs substrate using coplanar waveguide technology in the K -band [10], [11]. A 0.3- μm gate-length GaAs MESFET process was employed. The characteristic impedance of the transmission lines of the Wilkinson divider/combiner was set to 70 Ω , and that of both 45° delay line and 90° short stub was set to 50 Ω from (13). A photograph of the K -band MMIC 45° power divider/combiner is shown in Fig. 3. The chip size is 1.38 mm \times 0.875 mm. The measured characteristics are shown in Fig. 4, in which S_{21} and S_{31} are distribution characteristics, S_{11} is the reflection

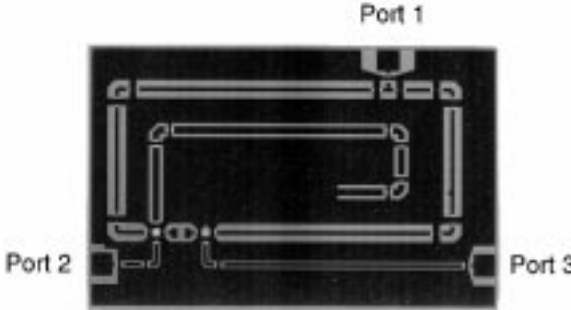


Fig. 3. Photograph of the K -band MMIC 45° power divider/combiner.

characteristic, and S_{32} is the isolation characteristic. A coupling loss of 4.0 ± 0.2 dB, and a return loss and an isolation of more than 19 dB were obtained over the 17–22-GHz frequency band. The phase difference between port 2 and port 3 was $45^\circ \pm 1^\circ$ in the same frequency range. Furthermore, in order to show the degree of improvement, the dotted line in Fig. 4 shows the calculated phase difference between port 2 and port 3 of a conventional 45° power divider/combiner designed with a center frequency of 20 GHz. Assuming that the electrical length of the delay line is in proportion to operating frequency, the calculated phase difference between port 2 and port 3 is 38.25° at 17 GHz and 49.5° at 22 GHz.

III. PARALLEL AMPLIFIER USING BROAD-BAND 45° DIVIDER/COMBINER

A. Power-Combining Circuit Configuration Requiring No Isolator

In millimeter-wave communication equipment, an isolator is sometimes inserted between an antenna and an RF circuit to solve the transmitter intermodulation problem, as shown in Fig. 5 [3], [4]. In the event that an interference signal with frequency f_I amplified by Transmitter 2 is transmitted via the antenna into Transmitter 1, which then amplifies the desired signal with frequency f_D , intermodulation ($mf_D + nf_I$, where $m, n = \pm 1, \pm 2, \dots$) is generated. This intermodulation is then transmitted from Transmitter 1. Although the isolator-insertion method is simple and effective, the following problems exist:

- 1) isolators are lossy and expensive;
- 2) isolators cannot be used in monolithic integration;
- 3) the shared area, which acts as a shield against magnetic fields, is large.

As a means of solving these problems, we have proposed a power-combining circuit configuration in which no isolator is required [2]. The circuit configuration of a parallel amplifier using a θ° divider/combiner is shown in Fig. 6(a). In this configuration, two unit amplifiers with nearly identical characteristics are set in parallel, with their input and output sides connected, respectively, to a θ° divider and combiner. The divider distributes half of the desired input signal with frequency f_D to each of the amplifiers, and the amplifiers then amplify their half of the divided signal. The two halves of the signal are then recombined in the combiner and are output.

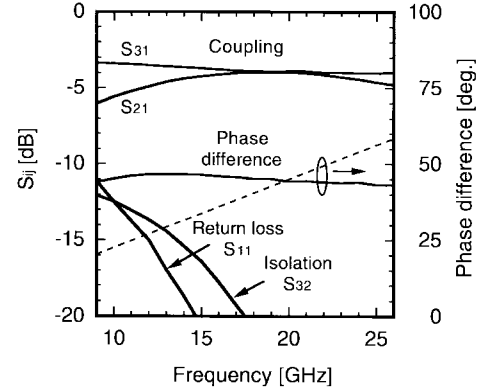


Fig. 4. Measured characteristics of the K -band MMIC 45° power divider/combiner.

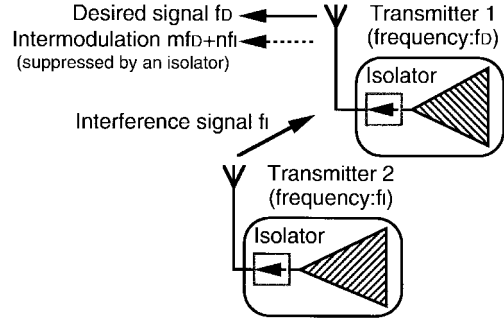


Fig. 5. Transmitter intermodulation problem.

Similarly, the circuit configuration of a parallel amplifier using a θ_1° divider/combiner and θ_2° dividers/combiners is shown in Fig. 6(b). In this configuration, four unit amplifiers with nearly identical characteristics are set in parallel. Fig. 6(c) shows a comparison of odd-order components emerging at the output ports of: 1) a parallel amplifier using a 0° divider/combiner; 2) a parallel amplifier using a 90° divider/combiner; 3) a parallel amplifier using a 45° divider/combiner; and 4) a parallel amplifier using 90° and 45° dividers/combiners. The parallel amplifier using the 0° divider/combiner cannot suppress any of the intermodulation. Although the interference signal with frequency f_I , the third-order intermodulation ($2f_D - f_I$), fifth-order intermodulation ($3f_I - 2f_D$), and seventh-order intermodulation ($4f_D - 3f_I$) are suppressed in the parallel amplifier using the 90° divider/combiner, it cannot suppress the third-order intermodulation ($2f_I - f_D$), fifth-order intermodulation ($3f_D - 2f_I$), and seventh-order intermodulation ($4f_I - 3f_D$). On the other hand, these last three components are suppressed in the parallel amplifier using the 45° divider/combiner.

From these results, it follows that a power-combining circuit configuration, which can cancel all of the transmitter intermodulation, can be obtained with the parallel amplifier using 90° and 45° dividers/combiners. Since all of the transmitter intermodulation is cancelled, it is not necessary for an isolator to be attached to the parallel amplifier.

B. Suppression of Transmitter Intermodulation

As mentioned above, under the ideal condition that the electrical characteristics of the 45° power divider/combiner, 90°

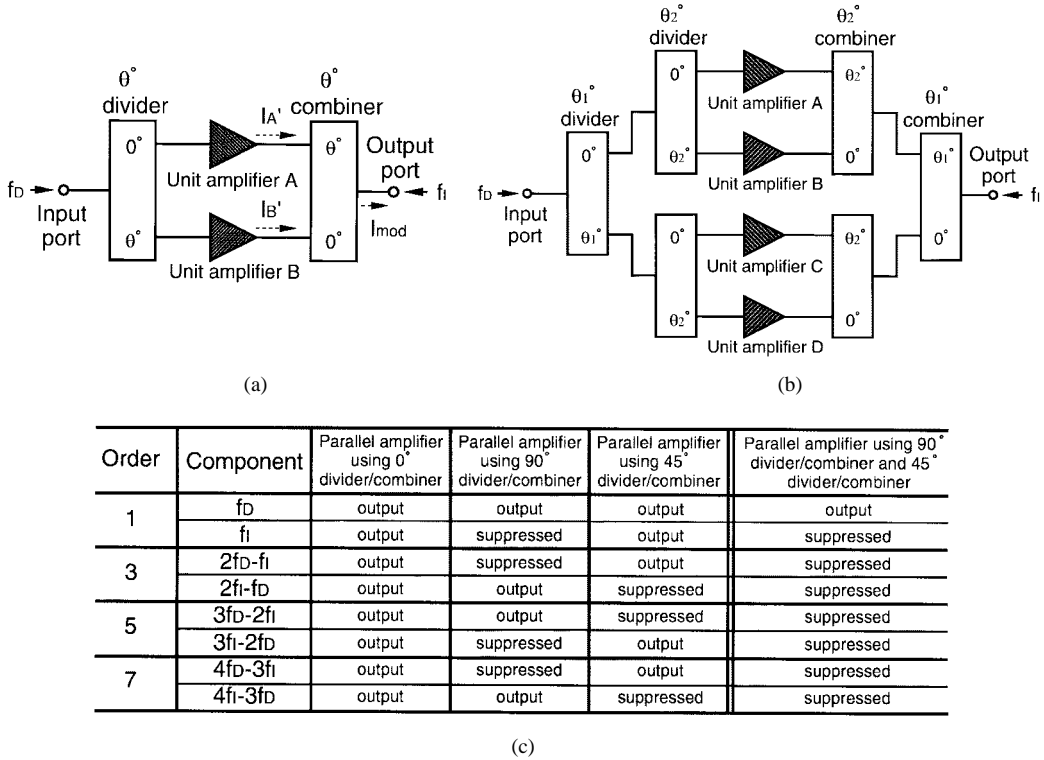


Fig. 6. Parallel amplifier. (a) Circuit configuration using θ° divider/combiner. (b) Circuit configuration using θ_1° divider/combiner and θ_2° dividers/combiners. (c) Comparison of odd-order components emerging at the output port.

power divider/combiner, and the unit amplifiers are perfect, the transmitter intermodulation is completely suppressed. However, since these have both amplitude and phase imbalance, the transmitter intermodulation cannot, in fact, be perfectly suppressed.

Therefore, we will give the relationship between the suppression of transmitter intermodulation and amplitude and/or phase imbalance in the parallel amplifier using the 45° or 90° divider/combiner by referring to Fig. 6(a). In this case, it is assumed that θ° means 45° or 90° . Unit amplifiers A and B have transmitter intermodulation currents, I'_A and I'_B , respectively. I'_A and I'_B are combined at the θ° combiner. If a phase and/or amplitude imbalance occurs, transmitter intermodulation current I_{mod} appears at the output port. I_{mod} is expressed as follows:

$$I_{\text{mod}} = \sqrt{I'_A{}^2 + I'_B{}^2 - 2I'_A I'_B \cos \alpha} \quad (14)$$

where α is the total phase imbalance. When the total amplitude imbalance is K dB, (14) is given by

$$I_{\text{mod}} = \sqrt{I'_A{}^2 + [10^{-(K/20)} I'_A]^2 - 2I'_A [10^{-(K/20)} I'_A] \cos \alpha} \quad (15)$$

where

$$K = \left| 20 \log \frac{I'_B}{I'_A} \right|. \quad (16)$$

We assume that the intermodulation suppression ratio R_{sup} is the ratio of I_{mod} to the total generated currents of transmitter intermodulation at the unit amplifiers A and B. Therefore, R_{sup} is given as shown in (17), at the bottom of the page.

The intermodulation suppression ratio versus phase and/or amplitude imbalance is shown in Fig. 7. Assuming that the performance of the unit amplifiers is equal, phase and/or amplitude imbalance is dominated by the θ° divider/combiner. For example, when $K = 0$ dB, in order to achieve an intermodulation suppression ratio over 30 dB, a phase imbalance of less than 3.6° is required within a desired frequency range. Thus, in order to obtain large suppression of the transmitter intermodulation, a broad-band 45° divider/combiner and broad-band 90° divider/combiner must be applied.

C. Experimental Parallel Amplifier Using Broad-Band 45° Divider/Combiner

For experimental purposes, we have fabricated a unit amplifier, parallel amplifier using the conventional 45° di-

$$R_{\text{sup}}(\text{dB}) = -20 \log \frac{\sqrt{I'_A{}^2 + [10^{-(K/20)} I'_A]^2 - 2I'_A [10^{-(K/20)} I'_A] \cos \alpha}}{I'_A + [10^{-(K/20)} I'_A]} \\ = -10 \log \frac{1 + 10^{-(K/10)} - 2[10^{-(K/20)}] \cos \alpha}{[1 + 10^{-(K/20)}]^2} \quad (17)$$

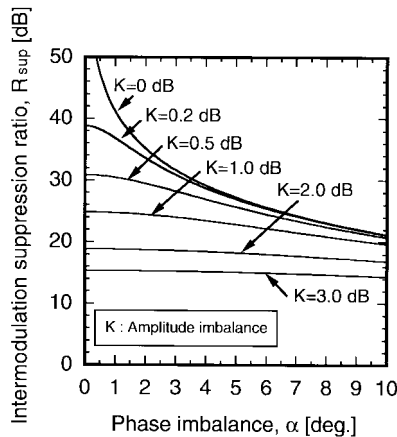


Fig. 7. Intermodulation suppression ratio versus phase and/or amplitude imbalance.

vider/combiner fabricated with simple delay line, and parallel amplifier using the proposed broad-band 45° divider/combiner in the K -band.

As an example, the circuit configuration and a photograph of the K -band MMIC parallel amplifier using the broad-band 45° divider/combiner are shown in Fig. 8. The chip size is $2.88 \text{ mm} \times 1.38 \text{ mm}$. The cascade-connected common-source FET amplifier configuration was employed for the unit amplifier. In order to reduce the chip size, high-impedance coplanar lines were used for the input and output matching circuits in the unit amplifier circuit. The drain voltages V_{d1} and V_{d2} were set at 3 V, and the drain currents I_{d1} and I_{d2} were set at I_{dss} . The total power consumption of the unit amplifier was about 200 mW.

Next, we have compared the frequency characteristics of transmitter intermodulation output levels by using the measurement circuit configuration shown in Fig. 9.

The measured frequency characteristics of the unit amplifier are shown in Fig. 10(a). The input powers of both the desired signal f_D and the interference signal f_I are about 3 dBm. It was found that the output power of the desired signal f_D is more than 9.5 dBm and that the third-order intermodulation ($2f_I - f_D$) is more than -30 dBm in the frequency range from 18 to 23 GHz. Since the typical small-signal gain of a unit amplifier is more than 14 dB from 19 to 22 GHz, the amplifier is fully saturated and the level of intermodulation can be ascertained easily.

The measured frequency characteristics of the parallel amplifier using the conventional 45° divider/combiner fabricated with simple delay line are shown in Fig. 10(b). The input powers of both the desired signal f_D and the interference signal f_I are about 7 dBm. It was found that the output power of the desired signal f_D is more than 11.5 dBm in the frequency range from 18 to 23 GHz and that the third-order intermodulation ($2f_I - f_D$) is less than -40 dBm in the frequency range from 19.8 to 22.2 GHz. Thus, to obtain an intermodulation suppression ratio R_{sup} of more than 14 dB, we are restricted to the latter frequency range, as can be seen by comparing Fig. 10(a) and (b).

The measured frequency characteristics of the parallel amplifier using the proposed broad-band 45° divider/combiner

is shown in Fig. 10(c). The input powers of both the desired signal f_D and the interference signal f_I are about 7 dBm. It was found that the output power of the desired signal f_D is more than 11.5 dBm in the frequency range from 18 to 23 GHz and that the third-order intermodulation ($2f_I - f_D$) is less than -40 dBm in the frequency range from 18.6 to 22.2 GHz. Thus, an intermodulation suppression ratio R_{sup} of more than 18 dB can be obtained in the latter frequency range, as can be seen by comparing Fig. 10(a) and (c).

As shown in Fig. 10(b) and (c), by using the proposed broad-band 45° divider/combiner, the third-order intermodulation ($2f_I - f_D$) can be more suppressed in a wider frequency range than it can in the case of using the conventional 45° divider/combiner with the simple delay line. Thus, with the proposed divider/combiner, a higher guaranteed R_{sup} can be obtained over a wider frequency range than with the conventional one.

In this experiment, we have used the MMIC configuration. Since the insertion loss of the fabricated K -band MMIC 45° divider/combiner is about 1 dB, the power-combining efficiency of this combiner is about 79% [12]–[14]. For example, in order to attain a power combining efficiency of more than 89%, the insertion loss must be suppressed to less than 0.5 dB. One possible solution to improve power-combining efficiency is to employ the microwave integrated circuit (MIC) configuration using a low-loss polyimide/alumina–ceramic multilayer substrate [15], [16]. Since this substrate enables compact arrangement of both the RF signal lines and the dc-bias lines, it is also applicable to millimeter-wave RF-module boards.

IV. SSB SHP MIXER USING BROAD-BAND 45° DIVIDER/COMBINER

A. Configuration of the SSB SHP Mixer Requiring No IF Switch

An SHP mixer using an antiparallel pair of diodes is suitable for millimeter-wave communication systems because it can reduce the number of multiplier-stages, requires no dc power, and can be used for both up- and down-conversion [17]. In practical use, an SSB mixer configuration is desired. In order to achieve low conversion loss and high image-rejection performance in an SSB mixer, its dividers/combiners have to be extremely accurate in amplitude and phase. A conventional type of SSB mixer for both up and down-conversion needs an LO in-phase divider and two quadrature hybrids at the IF and RF ports [18]. In this configuration, an IF switch, which takes up a large area, is conventionally used to change between transmission and reception.

We have previously proposed an SSB SHP mixer requiring no IF switch [5]. The configuration of this SSB SHP mixer is shown in Fig. 11. It consists of two SHP mixers, an LO 45° divider, IF 90° hybrid, and RF in-phase divider/combiner. In Fig. 11, the upper sideband (USB) is chosen as the desired signal. For up-conversion, an IF signal with frequency f_{IF} is input to the IF 90° hybrid, this is then divided and the two signals are fed into the mixers with 90° phase difference. LO power with frequency f_{LO} is input to the LO 45° divider,

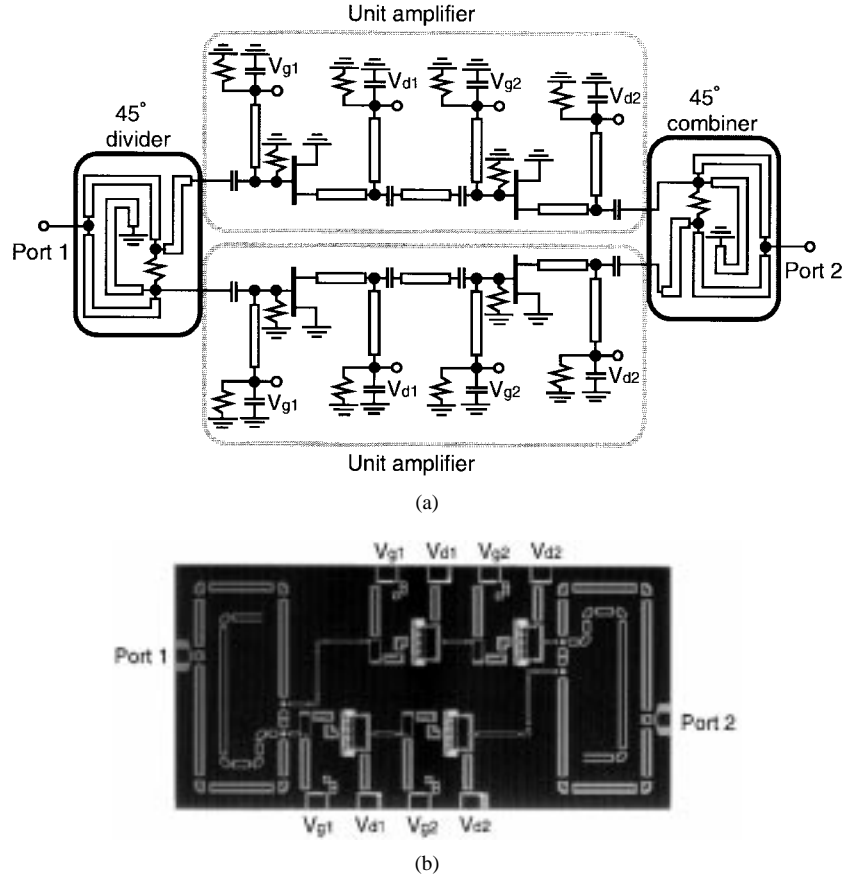


Fig. 8. *K*-band MMIC parallel amplifier using the broad-band 45° divider/combiner. (a) Circuit configuration. (b) Photograph.

this is then divided and the two LO powers are fed into the mixers with 45° phase difference. Then, the SHP mixers generate the up-converted signals, and the frequencies of their major components are described as $(2f_{\text{LO}} \pm f_{\text{IF}})$. Between the RF ports of the mixers, the up-converted USB components ($2f_{\text{LO}} + f_{\text{IF}}$) are in-phase with each other and lower sideband (LSB) components ($2f_{\text{LO}} - f_{\text{IF}}$) are out of phase, as shown in Fig. 11. Therefore, the desired up-converted USB signal appears at the output while the LSB signal is cancelled. For down-conversion, it also works as an image-rejection mixer similar to the case for up-conversion. However, as shown in Fig. 11, the down-converted USB component appears at the opposite port of the IF 90° hybrid. Therefore, the IF input and output ports can be connected directly with a modulator and a demodulator, respectively. Thus, the IF switch can be left out.

In this SSB mixer, the phase imbalance of LO power has a significant influence on the image-rejection ratio, while the amplitude imbalance of LO power has little effect on it, considering the LO power dependence of the SHP mixer. Thus, the broad-band 45° divider is needed for the LO 45° divider in order to obtain the good image-rejection ratio.

B. Experimental SSB SHP Mixer Using Broad-Band 45° Divider/Combiner

The circuit configuration of the *K*-band MMIC SSB SHP mixer using the proposed broad-band 45° divider/combiner is shown in Fig. 12(a). The SHP mixer has an IF low-pass

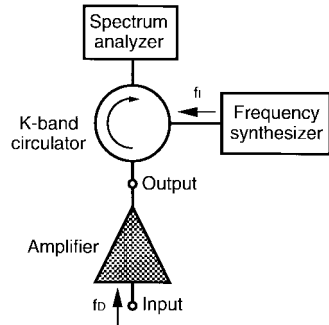


Fig. 9. Measurement circuit configuration.

filter and an RF high-pass filter to isolate RF and IF ports. In order to isolate the RF port from the LO port, the SHP mixer generally includes two stubs: an $\lambda_{\text{LO}}/4$ open stub and $\lambda_{\text{LO}}/4$ short stub. In order to make these stubs compact, each stub was fabricated by using the quasi-lumped method with shunt capacitors [5]. The RF in-phase divider/combiner was also fabricated with lumped elements to make its size compact. The LO 45° divider was realized with a proposed broad-band 45° divider/combiner. A photograph of the fabricated MMIC SSB SHP mixer is shown in Fig. 12(b). By using coplanar waveguide technology, the *K*-band mixer is integrated into a small area of 2.8 mm \times 1.28 mm. Each diode is realized by connecting source and drain of an FET, which has a gatewidth of 50 μm .

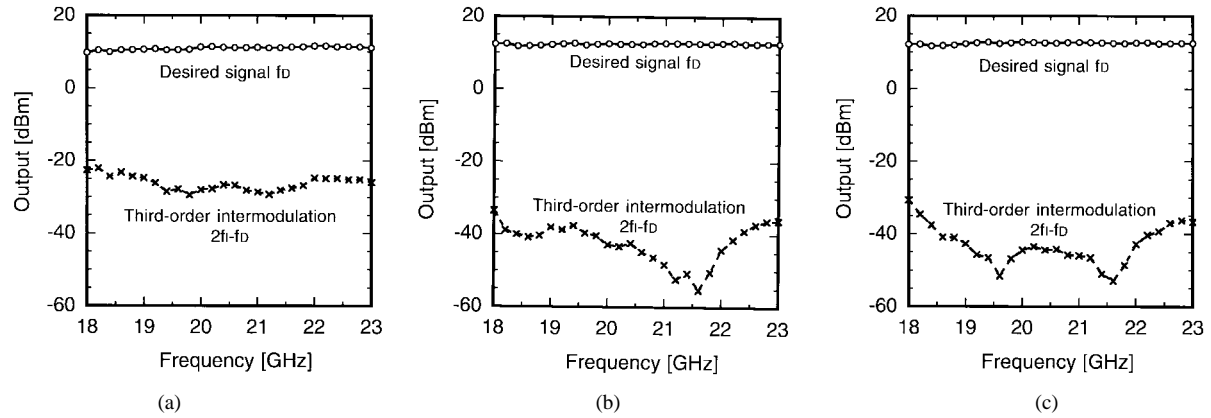


Fig. 10. Measured characteristics of the fabricated amplifier. (a) Unit amplifier. (b) Parallel amplifier using the 45° divider/combiner fabricated with simple delay line. (c) Parallel amplifier using the proposed broad-band 45° divider/combiner.

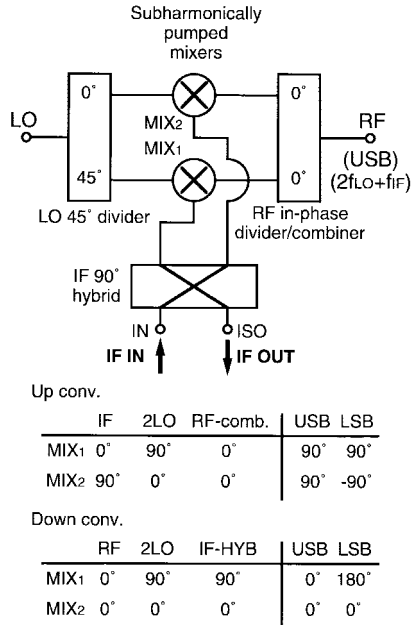


Fig. 11. Configuration of the proposed SSB SHP mixer.

Measured frequency characteristics of the fabricated SSB SHP mixer for up-conversion are shown in Fig. 13(a). IF is fixed at 0.14 GHz, and the input power level is set to -10 dBm. Conversion gain is more than -13 dB and image-rejection ratio is greater than 24 dB for LO frequencies from 11.375 to 13.125 GHz, which corresponds to RF frequencies from 22.89 to 26.39 GHz. As compared to the previously reported SSB mixer, the image-rejection ratio is improved by more than 5 dB in the same frequency range [5]. Measured frequency characteristics of the fabricated SSB SHP mixer for down-conversion are also shown in Fig. 13(b).

V. CONCLUSION

We have proposed millimeter-wave-band amplifier and mixer MMIC's using a broad-band 45° power divider/combiner. In the first stage of our work, we proposed the broad-band 45° power divider/combiner. The experimental MMIC broad-band 45° power divider/combiner was fabricated

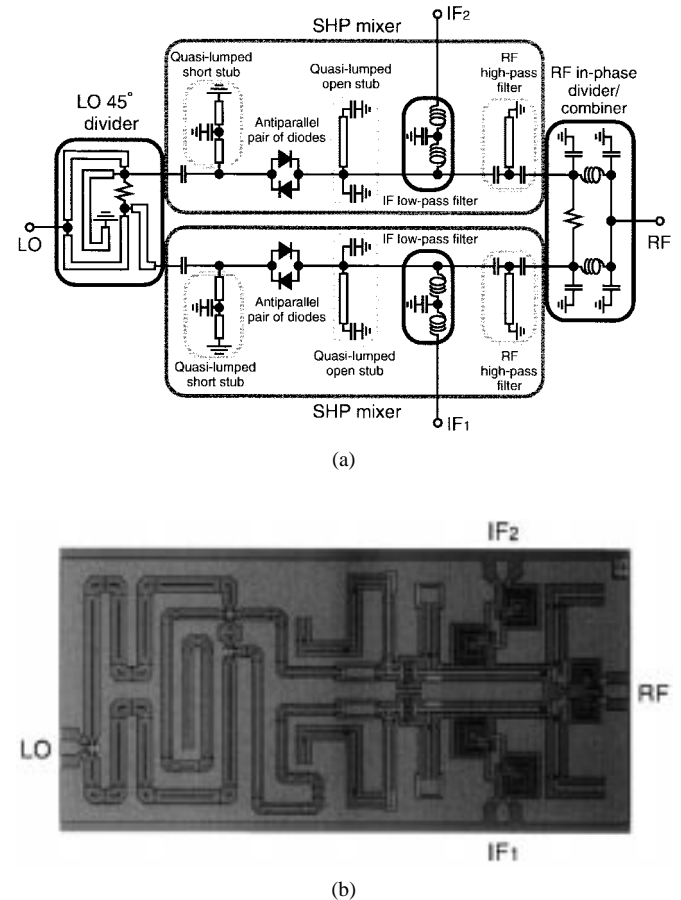


Fig. 12. *K*-band MMIC SSB SHP mixer. (a) Circuit configuration. (b) Photograph.

in the *K*-band. Next, we proposed the parallel amplifier using the broad-band 45° power divider/combiner and fabricated experimentally in the *K*-band. It was found that by using the proposed broad-band 45° divider/combiner, the third-order intermodulation ($2f_I - f_D$) can be more suppressed in wider frequency range than it can in the case of using the conventional 45° divider/combiner, and a higher R_{sup} can be obtained over a wider frequency range. Finally, we proposed an SSB SHP mixer using the broad-band 45° power

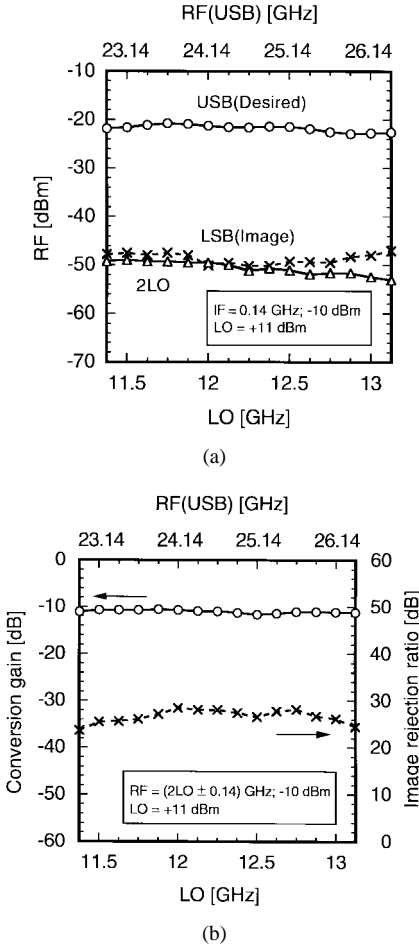


Fig. 13. Measured frequency characteristics of the K -band MMIC SSB SHP mixer for (a) up-conversion and (b) down-conversion.

divider/combiner. A good image-rejection ratio was obtained with the fabricated K -band SSB SHP mixer.

These circuits have the potential to significantly contribute to the miniaturization of millimeter-wave communication equipment.

ACKNOWLEDGMENT

The authors would like to thank Dr. T. Murase, A. Minakawa, and Y. Yamaguchi for their helpful information and encouragement.

REFERENCES

- [1] H. Tokuda, "Technology trends of millimeter-wave HEMT MMIC's," in *IEICE APMC'94 Workshop Dig.*, vol. WS1-3, Tokyo, Japan, Dec. 1994, pp. 19-24.
- [2] H. Hayashi, H. Okazaki, A. Kanda, T. Hirota, and M. Muraguchi, "A novel power combining configuration without using an isolator," in *IEEE TSMMW'97 Dig.*, vol. 4-2, Hayama, Japan, July 1997, pp. 40-41.
- [3] Y. Okumura and M. Shinji, *Basis of Mobile Communication*. Tokyo, Japan: IEICE, 1986 (in Japanese).
- [4] R. Kawasaki and T. Habuka, "Reduction of the intermodulation products of transmitters using a balanced amplifier with a pair of quadrature hybrids," vol. MW78-82, IEICE, Japan, Tech. Rep. 143, pp. 55-61, 1978 (in Japanese).
- [5] H. Okazaki and Y. Yamaguchi, "Wide-band SSB subharmonically pumped mixer MMIC," in *IEEE MTT-S Symp. Dig.*, vol. WE4B-1, Denver, CO, 1997, pp. 1035-1038.

- [6] I. Toyoda, T. Hirota, T. Hiraoka, and T. Tokumitsu, "Multilayer MMIC branch-line coupler and broad-side coupler," in *IEEE Microwave Millimeter-Wave Monolithic Circuits Symp. Dig.*, Albuquerque, NM, June 1992, pp. 79-82.
- [7] S. Banba and H. Ogawa, "Multilayer MMIC directional couplers using thin dielectric layers," *IEEE Trans. Microwave Theory Tech.*, vol. 43, pp. 1270-1275, June 1995.
- [8] H. Okazaki and T. Hirota, "Multilayer MMIC broad-side coupler with a symmetric structure," *IEEE Microwave Guided Wave Lett.*, vol. 7, pp. 145-146, June 1997.
- [9] T. Tokumitsu, K. Nishikawa, K. Kamogawa, I. Toyoda, and K. Nishimura, "Three-dimensional technology and application to millimeter-wave MMIC's," in *IEEE TSMMW'97 Dig.*, vol. 4-4, Hayama, Japan, July 1997, pp. 44-45.
- [10] M. Muraguchi, T. Hirota, A. Minakawa, K. Ohwada, and T. Sugeta, "Uniplanar MMIC's and their applications," *IEEE Trans. Microwave Theory Tech.*, vol. 36, pp. 1896-1901, Dec. 1988.
- [11] I. Wolff, "Design rules and realization of coplanar circuits for communication applications," in *Proc. 23rd EuMC*, Madrid, Spain, Sept. 1993, pp. 36-41.
- [12] J. L. B. Walker, *High-Power GaAs FET Amplifiers*. Norwood, MA: Artech House, 1993, pp. 298-301.
- [13] K. J. Russell, "Microwave power combining techniques," *IEEE Trans. Microwave Theory Tech.*, vol. MTT-27, pp. 472-478, May 1979.
- [14] K. Chang and C. Sun, "Millimeter-wave power-combining techniques," *IEEE Trans. Microwave Theory Tech.*, vol. MTT-31, pp. 91-107, Feb. 1983.
- [15] H. Hayashi, M. Muraguchi, Y. Umeda, and T. Enoki, "A high- Q broadband active inductor and its application to a low-loss analog phase shifter," *IEEE Trans. Microwave Theory Tech.*, vol. 44, pp. 2369-2374, Dec. 1996.
- [16] M. Nakatsugawa, A. Kanda, H. Okazaki, K. Nishikawa, and M. Muraguchi, "Line-loss and size-reduction techniques for millimeter-wave RF front-end boards by using a polyimide/alumina-ceramic multilayer configuration," in *IEEE MTT-S Symp. Dig.*, vol. WE2A-3, Denver, CO, 1997, pp. 509-512.
- [17] M. Cohn, J. E. Degenford, and B. A. Newman, "Harmonic mixing with an antiparallel diode pair," *IEEE Trans. Microwave Theory Tech.*, vol. MTT-23, pp. 667-673, Aug. 1975.
- [18] S. A. Maas, *Microwave Mixers*, 2nd ed. Norwood, MA: Artech House, 1993, pp. 280-284.

Hitoshi Hayashi (M'94) was born in Nagoya, Japan, in 1966. He received the B.Eng. and M.Eng. degrees in electronics engineering from the University of Tokyo, Tokyo, Japan, in 1990 and 1992, respectively.

In 1992, he joined NTT Radio Communication Systems Laboratories, Yokosuka, Japan, where he had been involved in research on MMIC's. He is currently with NTT Wireless Systems Laboratories, Yokosuka, Japan, where he is engaged in the development of microwave amplifiers.

Mr. Hayashi is a member of the Institute of Electronics, Information, and Communication Engineers (IEICE), Japan. He was the recipient of the 1998 Young Engineer Award given by the IEICE.



Hiroshi Okazaki (A'94) was born in Okayama, Japan, in 1965. He received the B.E. and M.E. degrees from Osaka University, Osaka, Japan, in 1988 and 1990, respectively.

In 1990, he joined NTT Radio Communication Systems Laboratories, Yokosuka, Japan, where he was involved in the investigation of low power-consumption solid-state power amplifiers (SSPA's) for earth stations. He is currently a Research Engineer at NTT Wireless Systems Laboratories, Yokosuka, Japan, where he is engaged in research on microwave-circuit techniques for monolithic integration.

Mr. Okazaki received the Young Engineer Award from the Institute of Electronics, Information, and Communication Engineers (IEICE), Japan, in 1997.



Atsushi Kanda (M'95) was born in Tokyo, Japan, in 1963. He received the B.E. degree in applied physics from Waseda University, Tokyo, Japan, and the M.E. degree in information processing from the Tokyo Institute of Technology, Tokyo, Japan, in 1988 and 1990, respectively.

In 1990, he joined NTT Radio Communication Systems Laboratories, Yokosuka, Japan, where he had been engaged in the investigation of mobile phone equipment. He is currently involved in research and development of MMIC's for communication systems.

Mr. Kanda is a member of the Institute of Electronics, Information, and Communication Engineers (IEICE), Japan.



Tetsuo Hirota (M'87) was born in Takaoka, Japan, in 1956. He received the B.E., M.E., and D. Eng. degrees in electronics from Kyoto University, Kyoto, Japan, in 1979, 1981, and 1996, respectively.

In 1981, he joined NTT Electrical Communication Laboratories, where he was involved in the research and the development of MIC's for communication systems, including nonlinear FET circuits and uniplanar MMIC's. From 1991 to 1992, he was at the University of California at Los Angeles as a Visiting Scholar. Since 1997, he has been with NTT Mobile Communications Network Inc., Tokyo, Japan.

Dr. Hirota is a member of the Institute of Electronics, Information, and Communication Engineers (IEICE), Japan.



Masahiro Muraguchi (S'80–M'83) was born in Kanazawa, Japan, on May 23, 1955. He received the B.Eng. degree in electrical engineering from the Nagoya Institute of Technology, Nagoya, Japan, in 1978, and the M.Eng. and Ph.D. degrees in physical electronics engineering from the Tokyo Institute of Technology, Tokyo, Japan, in 1980 and 1983, respectively.

In 1983, he joined the NTT Atsugi Electrical Communications Laboratories, Nippon Telegraph and Telephone Corporation, where he was involved in the design and fabrication of GaAs MMIC's. He is currently engaged in research and development work on MMIC's for wireless communications at the NTT Wireless Systems Laboratories, Kanagawa, Japan, where he is the Leader of the Microwave Circuit Group. He has been on the Editorial Committee of *IEICE Transactions on Electronics* as an associate editor since 1994.

Dr. Muraguchi is a member of the Institute of Electronics, Information, and Communication Engineers (IEICE), Japan. He was awarded the Ichimura Prize by the New Technology Development Foundation in 1994.